



Effect of elevated carbon dioxide and nitric oxide on the physiological responses of two green algae, *Asterarcys quadricellulare* and *Chlorella sorokiniana*

Prachi Varshney^{1,2,3,4} · John Beardall³ · Sankar Bhattacharya⁴ · Pramod P. Wangikar^{2,5,6}

Received: 20 April 2019 / Revised and accepted: 9 October 2019 / Published online: 2 December 2019
© Springer Nature B.V. 2019

Abstract

Algae have the potential to capture carbon dioxide (CO₂) and nitric oxide (NO) from flue gases. However, the effects of high concentrations of these gases on the photophysiology of algae are poorly understood. To that end, we used the techniques of chlorophyll fluorescence to study the effect of industrially relevant levels of CO₂ and NO on the photophysiology of two green microalgae, *Asterarcys quadricellulare* and *Chlorella sorokiniana*, that are tolerant to these gases. Measurements of maximum quantum yield (F_v/F_m) and maximum relative electron transport rate ($rETR_{max}$) show an enhanced performance of photosystem II (PSII) under high CO₂ levels. In *C. sorokiniana*, high CO₂ stimulated non-photochemical quenching (NPQ), while the opposite effect was observed in *A. quadricellulare*. Light-saturated photosynthetic rates (P_{max}) of both species were highest at 10% CO₂. Further, the tested levels of NO did not show adverse effect on the performance of PSII. OJIP chlorophyll fluorescence transients suggest that in *C. sorokiniana*, the energetic communication between PSII units declined at 15% CO₂. However, in *A. quadricellulare*, this decline was visible even at 10% CO₂ with complete inhibition of cell growth at 15% v/v. Overall, our results suggest that although photosynthesis was regulated differently in the two microalga, both species exhibited enhanced PSII performance under reasonably high levels of CO₂ and NO. Thus, the two species are potential candidates for bio-fixation of CO₂ and NO from flue gases.

Keywords CO₂ tolerance · Chlorophyll *a* fluorescence · Physiological stress · Non-photochemical quenching · PSII heterogeneity · Photosynthetic rates

Introduction

Flue gas is an assortment of carbon dioxide (CO₂), nitrogen oxides (NO_x), sulfur oxides (SO_x), carbon monoxide (CO), and particulate matter. Nitric oxide (NO) is the main component of NO_x in the flue gas (>90%). Both

CO₂ and NO are considered as major greenhouse components and are viewed as potential agents of global climate change. While CO₂ is a source of carbon for algal mass culture, NO when dissolved in water forms nitrite and could be an effective N-source for algae (Zhang et al. 2015). Consequently, there has been significant interest

Electronic supplementary material The online version of this article (<https://doi.org/10.1007/s10811-019-01950-2>) contains supplementary material, which is available to authorized users.

✉ Pramod P. Wangikar
wangikar@iitb.ac.in

¹ IITB-Monash Research Academy, Indian Institute of Technology Bombay, Powai, Mumbai, Maharashtra, India

² Department of Chemical Engineering, Indian Institute of Technology Bombay, Powai, Mumbai, Maharashtra, India

³ School of Biological Sciences, Monash University, Clayton, Melbourne, Victoria, Australia

⁴ Department of Chemical Engineering, Monash University, Clayton, Melbourne, Victoria, Australia

⁵ DBT-Pan IIT Centre for Bioenergy, Indian Institute of Technology Bombay, Powai, Mumbai, Maharashtra, India

⁶ Wadhvani Research Centre for Bioengineering, Indian Institute of Technology Bombay, Powai, Mumbai, Maharashtra, India

in developing strategies for the photosynthetic capture of CO₂ and NO from flue gases using microalgal cultures (Yoshihara et al. 1996; Chiu et al. 2011; Zhao et al. 2015; Ma et al. 2019). However, the high levels of these greenhouse components may result in stress to the microalgae (Chiu et al. 2008, 2009, 2011). The stress response of these photosynthetic microorganisms also depends upon the duration of exposure of the culture to the potentially toxic gases (Makino and Mae 1999; Nagase et al. 2001). The concentration of CO₂ influences not only the growth rate, morphology, and activity of proteins involved in carbon acquisition by CO₂-concentrating mechanisms (CCMs) but also the overall photosynthetic rates and capacity, as well as the organization of the photosynthetic apparatus and its performance (Spalding et al. 1984; Pierangelini et al. 2014a; Li et al. 2015). Therefore, besides understanding the growth and macromolecular composition of algae under elevated levels of CO₂ and NO, it is also important to study the physiological effects of high concentrations of these gases in order to better exploit algal species for flue gas treatment and possible biofuel production.

Chlorophyll (Chl) *a* fluorescence analysis is a rapid, powerful, and non-invasive technique that is widely used in physiological and ecophysiological studies of plants and algae (Stirbet et al. 1998; Baker 2008). At room temperature, the fluorescence signal of plants and algae occurs in the spectral region of 680–740 nm and mainly originates from photosystem II (PSII) (Spalding et al. 1984; Maxwell and Johnson 2000; Strasser et al. 2004). The most pervasive use of Chl *a* fluorescence in microalgae is in examining the performance of PSII photochemistry, linear electron flow and CO₂ assimilation (Baker 2008). Another application of Chl *a* fluorescence is in the monitoring of the structural and conformational changes in photosystems that accompany the photosynthetic reactions (Strasser et al. 2004). It is widely acknowledged that PSII in the chloroplasts of green algae, as well as in higher plants, is heterogeneous in relation to both the antenna (α and β heterogeneity) and reducing sites of P680 (Q_B and non- Q_B), and the reaction center chlorophylls of PSII (Guenther and Melis 1990). The antenna heterogeneity is defined by the biphasic Chl *a* fluorescence induction kinetics of PSII activity, which arises as the reaction centers (RC) progressively close upon photoreduction of the primary quinone electron acceptor of PSII (Q_A). The biphasic nature of the kinetics confirms the existence of two types of PSII centers in the chloroplast. The first phase, PSII α (fast phase), is shown by the nonlinearity of a semi-logarithmic plot of fluorescence versus time and corresponds to sigmoidal induction kinetics. This sigmoidicity can be explained by the presence of α centers in a static pigment bed that allows energy

transfer between PSII units. The second phase, PSII β (slow phase), is reflected by the linearity of the semi-logarithmic plot of fluorescence versus time and corresponds to exponential induction kinetics. The exponentiality of β centers can be explained by their existence as “separate packages” in which energy transfer from closed to open centers is not possible (Black et al. 1986). The rate difference between PSII α and PSII β corresponds to their different light-harvesting antenna sizes. In mature chloroplasts of wild-type vascular plants, PSII α accounts for 75–80% of all PSII centers and PSII β accounts for the remaining 20–25% (Guenther and Melis 1990).

Although the effects of CO₂ and NO on the growth, biochemical composition, and CO₂ concentrating mechanism (CCM) activity in algae have been widely studied (Nagase et al. 1997; Basu et al. 2013; Varshney et al. 2015, 2016, 2018), the effect of high levels of these gases on the performance of the photosynthetic apparatus and PSII heterogeneity in algae has not been adequately investigated (Spalding et al. 1984; Iwasaki et al. 1996; Bhola et al. 2016). Also, there can be large variability in the acclimation of photosynthetic characteristics and the defense strategies adopted by different algal species in response to certain environmental stress, and that may not always match the theoretical expectation (Vincent and Roy 1993; Ainsworth and Rogers 2007). Hence, in this study, we focussed on the changes in the functional and structural aspects of the photosynthetic apparatus of two high-CO₂ and NO-tolerant freshwater green algae upon their prolonged exposure to industrial levels of CO₂ and NO, by using *in vivo* Chl *a* fluorescence technique (PAM, FFI, and OJIP analysis). We also measured the light-saturated photosynthetic oxygen evolution and dark respiration rates (P_{\max} and R_d) of these species in response to elevated levels of CO₂ and NO to better understand the effects of these gases on the photosynthetic performance of algae.

Materials and methods

Microorganisms and cultivation conditions

Two freshwater green algae species, *Asterarcys quadricellulare* and *Chlorella sorokiniana*, which were isolated from steel plant effluent water, were used in this study. These species were characterized phylogenetically and morphologically in a previous study (Varshney et al. 2018). The species were grown in Bold's Basal medium (BB) at pH 6.8 in a Photo Multi-Cultivator MC 1000-OD (Photon System Instruments, Czech Republic) and during experiments the pH of the cultures was not controlled.

The details of the photobioreactor setup have been specified in the previous study (Varshney et al. 2018). The BB media was prepared according to the medium recipe reported by the Culture Collection of Algae and Protozoa (CCAP) (<https://www.ccap.ac.uk/media/documents/BB.pdf>). The temperature of the cultivation vessels was maintained at 37 °C and a peak light intensity of 250 $\mu\text{mol photons m}^{-2} \text{s}^{-1}$ was applied in a 14:10 light-dark (LD) cycle following a 14 h sine function. All the experiments were performed on triplicate-independent cultures and the initial cell concentration of 0.6×10^6 cells mL^{-1} was maintained in each vessel. Since the maximum working volume in each vessel was only 85 mL, the cultures were grown in semi-continuous culture mode, so that sufficient samples were available for different analysis. Initially, the sampling was performed in mid-exponential phase and the cultures were diluted to the previous day's cell concentration. Once the sampling in mid-exponential phase was completed, the cultures were allowed to grow into stationary phase and the same sampling procedure was repeated.

The typical concentration of CO_2 in the selected steel plant flue gas was 15–20% v/v, thus three gradually increasing concentrations of CO_2 , namely 5, 10, and 15% v/v, were prepared by mixing U.H.P. grade pure CO_2 with compressed air. The filtered compressed air was used to grow cultures in ambient CO_2 conditions (0.04% CO_2). Since it has already been shown that *A. quadricellulare* does not grow at 15% CO_2 (Varshney et al. 2018), this alga was tested only up to a CO_2 level of 10% v/v. Further, since both the species exhibited maximum growth rate at 5% CO_2 , this level of CO_2 was chosen for further experiments using two levels of simulated flue gas, namely 5% CO_2 + 80 ppm NO and 5% CO_2 + 160 ppm NO, obtained by blending gas from a cylinder that contained 500 ppm NO in N_2 , with CO_2 and compressed air. While *C. sorokiniana* was tested for both blends of CO_2 and NO, *A. quadricellulare* was only tested under 5% CO_2 + 80 ppm NO. The gas mixtures were bubbled through the cultivation vessels at a fixed aeration rate of 0.45 vvm (gas volumetric flow rate per unit volumetric culture medium per minute). The initial inoculum was taken from log-phase stock cultures that were prepared by growing cells under the same conditions for at least 2 weeks; the cells underwent regular sub-culturing at every third or fourth day when they were in their late exponential phase.

Except for flash fluorescence induction (FFI) curves, all the other analyses presented here are based only on measurements performed on mid-exponential phase samples. The effect of NO was assessed through the phytoplankton pulse amplitude-modulation fluorometry (Phyto-PAM) analysis and photosynthetic oxygen evolution measurements.

Rapid light curve measurements

The photosynthetic performance of algae was examined by chlorophyll fluorescence measurements of PSII activity via rapid light curves (RLCs) generated using a pulse amplitude modulated fluorimeter (Phyto-PAM, Heinz Walz, Germany). Briefly, a 3.5 mL algal sample was carefully collected to minimize perturbation to the dissolved gases and dark acclimated for 15 min, which is usually sufficient in dense microalgal cultures (Masojídek et al. 2010). The sample was then exposed to a weak modulated measuring light beam at an intensity that did not excite the PSII reaction centers (i.e., low enough to avoid photochemistry) and resulted in a minimal level of fluorescence (F_o). Further, the sample was exposed to a short (0.2 s) saturating beam of very bright red light (655 nm), which resulted in the maximum reduction of Q_A , and the maximal fluorescence level F_m was attained. The difference between F_m and F_o was defined as variable fluorescence, F_v , and the ratio of F_v/F_m was used to calculate the maximum quantum yield of photosynthetic energy conversion in PSII. The RLCs were constructed by exposing culture samples to 20 increasing irradiance levels from 8 to 610 $\mu\text{mol photons m}^{-2} \text{s}^{-1}$. Each light exposure was for 30 s and was followed by a saturating pulse to allow the determination of effective quantum yield under actinic light (non-modulated light that is absorbed by the photosynthetic apparatus and that will drive photosynthesis). The relative electron transport rate was calculated from the effective quantum yield and the incident photosynthetically active radiation (PAR), using Eq. (1):

$$rETR = \text{Yield} \times \text{PAR} \times A \times \text{Fraction}_{PSII} \quad (1)$$

where A is the absorbance that is assumed to be 0.84 for higher plant leaves, which means that 84% of the incident PAR is absorbed by the leaves. Similarly, Fraction_{PSII} for plant leaves is taken as 0.5, under the assumption that 50% of the absorbed PAR is distributed to PSII (that is, absorbed energy is evenly distributed between the two photosystems, PSI and PSII). Since the absorbance was not measured but was assumed, ETR is here expressed as relative values (rETR) (Baker 2008). RLCs are also used to calculate the light harvesting efficiency (α), light-saturated rETR ($rETR_{\text{max}}$), and the light intensity at which rETR saturates (I_k). The α represents the initial slope of the rETR versus light curve, and I_k corresponds to the PAR value that is located at the intersection of the initial slope (α) and a line that is parallel to the PAR axis and originates from $rETR_{\text{max}}$ (Fig. 1, Supplementary Information). Numerically, I_k is derived from the expression $rETR_{\text{max}}/\alpha$ (Ralph and Gademann 2005). All the above parameters were calculated by the in-built PhytoWin software that provides routines for fitting the RLC parameters using mechanistic model of Eilers and Peeters (1988). The light intensity at which rETR saturated was then used to obtain

the maximum photosynthetic rate (P_{\max}) from the oxygen evolution experiments.

Non-photochemical quenching analysis

The Phyto-PAM fluorimeter was also used to perform analysis of non-photochemical quenching (NPQ), which is an estimation of the capacity of cells to dissipate excess light energy as heat (Kalaji et al. 2014). A 15 min dark-adapted sample was exposed to a weak measuring light beam and then to a saturating light pulse to determine the values of F_o and F_m , respectively. The measurement was continued by switching on an actinic light source of an intensity of $480 \mu\text{mol photons m}^{-2} \text{s}^{-1}$ (chosen from RLCs to be supra-saturating for electron transport) for 10 min to induce photosynthesis, during which a 20 s cycle of saturating red pulses was applied until a stable value of maximum fluorescence yield in the light (F_m') was attained. We used the Stern-Volmer approach (Eq. 2) as the NPQ values generated by the fluorometer software as part of the data generation during RLC can sometime be less reliable as they are taken over a short time frame rather than at a steady state.

$$NPQ = \frac{F_m}{F_m'} - 1 \quad (2)$$

Photosynthetic oxygen evolution measurements

The rates of light-saturated photosynthetic oxygen evolution (P_{\max}) and dark respiration (R_d) were measured using a Clark-type oxygen electrode (Hansatech, UK) at 37°C . For *A. quadricellulare*, 15×10^6 cells, and for *C. sorokiniana*, 30×10^6 cells were harvested from the culture and resuspended in 2.0 mL of fresh culture medium that was buffered with 20 mM HEPES at pH 6.8; the medium contained 2.0 mM inorganic carbon (NaHCO_3). Samples were placed into the O_2 electrode chamber and were continuously stirred at 75 rpm by a magnetic flea that was placed within the electrode chamber. The cell suspension was bubbled with N_2 gas to reduce the O_2 concentration to 20% of air saturation (Yang and Gao 2003). The cells were then dark acclimated for 20 min or until the oxygen concentration decreased at a stable rate and the ultimate 3 min of this incubation was used to measure the R_d . The saturating light intensity, which provided $r\text{ETR}_{\max}$, as determined from PAM RLC measurements was then applied to the samples to obtain P_{\max} . The rates of oxygen evolved or consumed by the cells were calculated by the Oxygraph Plus software. The gross photosynthetic rate (Gross P) was calculated by correcting the net exchange rate of O_2 (P_{\max}) for the absolute value of dark respiration rate (R_d) by using Eq. (3) (Henley 1995).

$$\text{Gross P} = \text{Net } P_{\max} + R_d \quad (3)$$

where R_d is expressed as (positive) oxygen consumption.

Flash fluorescence induction curves

Flash fluorescence induction (FFI) curves were generated using a double-modulation kinetic fluorimeter FL-3000 (Photon Systems Instruments, Czech Republic). Briefly, samples containing 10×10^6 cells of *A. quadricellulare* or 40×10^6 cells of *C. sorokiniana* were harvested and dark acclimated for 15 min. A single turnover saturating flash of 100% light intensity (equivalent to $208,000 \mu\text{mol photons m}^{-2} \text{s}^{-1}$) (Nedbal et al. 1999; Dao and Beardall 2016a) was applied for 50 μs , with the detector sensitivity set at 5%. Based on the equations of Lavergne and Trissl (1995), the rise of fluorescence after applying the saturating flash was numerically fitted to a theoretical fluorescence induction curve. This was done in order to calculate minimum fluorescence (F_o), maximum fluorescence (F_m), functional absorption cross-section (σPSII), sigmoidicity (J), PSII α /PSII β stoichiometry, and reaction center excitation rates (Lavergne and Trissl 1995; Nedbal et al. 1999; Vinet and Zhedanov 2011).

Chl *a* fluorescence transients (OJIP test)

The progressive reduction of the electron transport chain (ETC) leads to the polyphasic rise of Chl *a* fluorescence from F_o to F_m , in four major steps, namely O, J, I, and P, which are known as OJIP transient (Fig. 2, Supplementary Information). These transients yield information about the quantitative characteristics of PSII and the heterogeneity that is involved in the reduction of the PQ pool (Antal and Rubin 2008; Markou et al. 2017). Their shape is a sensitive indicator of changes in different environmental conditions such as light intensity, temperature, CO_2 concentration, and chemical influences etc. (Strasser et al. 2004). For our experiments, we recorded these transients by using the same double-modulation kinetic fluorimeter FL-3000 as described in the previous section. To generate the curves, a multiple turnover flash at 100% light intensity was applied to the sample that had been dark acclimated for 15 min. Measurements were conducted for 1 s and were recorded at every 10 μs up to 2 ms and then at every 1 ms until 1 s. The fluorescence intensity was observed to increase from a minimum value $F_o = F_{50\mu\text{s}}$ (O-step), via two intermediate steps, $F_j = F_{2\text{ms}}$ (J-step) and $F_i = F_{30\text{ms}}$ (I-step) to a maximum value, F_m (P-step). It has been reported that under stress conditions when the oxygen-evolving complex (OEC) of PSII is completely destroyed, an earlier step at approximately 300 μs develops in the fluorescence rise from O-P and is labeled as the K-step (Schmitz and Maldonado-Rodriguez 2001; Strasser et al. 2004; Zhao et al. 2008). To standardize the results, all the fluorescence values were normalized to F_o . By using F_o , F_j , F_i , and F_m values, the key JIP-test parameters were derived by following the equations of Strasser et al. (2004).

The relative variable fluorescence values at step *K* and *J* were calculated according to Eq. (4) and Eq. (5).

$$V_K = \frac{F_K - F_0}{F_M - F_0} = \frac{F_{300\mu s} - F_0}{F_M - F_0} \tag{4}$$

$$V_J = \frac{F_J - F_0}{F_M - F_0} = \frac{F_{2ms} - F_0}{F_M - F_0} \tag{5}$$

The maximum quantum yield of primary photochemistry (ϕ_{P0}) was calculated using Eq. (6). It is considered as a synonym of efficiency and is the ratio of the total energy flux that is trapped by the PSII RCs (when all the RCs are open) and is used for photochemistry at time zero (TR_0) to the total energy influx that is absorbed by the antenna pigments (ABS) (Fig. 3, Supplementary Information).

$$\phi_{P0} = \frac{TR_0}{ABS} = \frac{F_V}{F_M} = \frac{F_M - F_0}{F_M} \tag{6}$$

Furthermore, the probability (Ψ_0) that a trapped exciton moves an electron into the ETC beyond Q_A^- was calculated by Eq. (7). It is the ratio of trapped excitation energy that goes beyond Q_A oxidation (ET_0) to the energy flux that was trapped by the PSII RC (TR_0).

$$\Psi_0 = \frac{ET_0}{TR_0} = 1 - V_J \tag{7}$$

The net rate of closure of RCs was calculated from the initial slope of fluorescence transient (M_0) by using Eq. (8), where trapping flux (TR_0) increases the number of closed RCs and electron flux (ET_0) decreases it.

$$M_0 = 4 \times V_K = \frac{TR_0}{RC} - \frac{ET_0}{RC} \tag{8}$$

The performance index (PI, on absorption basis), which is a product of the terms that represent the energy bifurcations in PSII, was calculated using Eq. (9)

$$PI_{ABS} = \frac{RC}{ABS} \times \frac{\phi_{P0}}{1 - \phi_{P0}} \times \frac{\Psi_0}{1 - \Psi_0} \tag{9}$$

The *hyperbola constant* or *curvature constant* (C_{HYP}) that is equivalent to the sigmoidicity parameter “ J ”, and the *overall grouping probability* (p_{2G}) were calculated according to Eq. (10) and Eq. (11). C_{HYP} is a product of energy fluxes at two extremes (with all RCs open or closed) and the probabilities of all types of energetic communication among the PSII pools, which is commonly known as *overall grouping probability* (p_{2G}).

$$J = C_{HYP} = \left(\frac{F_M}{F_0} - 1 \right) \times p_{2G} \tag{10}$$

$$p_{2G} = \frac{W_{E,100\mu s} - W_{100\mu s}}{W_{100\mu s} \times (1 - W_{E,100\mu s} \times V_J) \times V_J} \times \frac{F_0}{F_M - F_0} \tag{11}$$

where,

$$W_{E,100\mu s} = 1 - (1 - W_{300\mu s})^{1/5} \tag{11a}$$

$$W_{100\mu s} = \frac{F_{100\mu s} - F_{50\mu s}}{F_{2\mu s} - F_{50\mu s}} \tag{11b}$$

$$W_{300\mu s} = \frac{F_{300\mu s} - F_{50\mu s}}{F_{2\mu s} - F_{50\mu s}} \tag{11c}$$

Finally, the specific energy flux (per fully active, that is, Q_A reducing PSII RC) of absorption (ABS), was calculated using Eq. (12). It is an estimation of the average amount of absorbing chlorophylls per (active) RC, that is, the apparent antenna size (Strasser et al. 2004; Zhang et al. 2010a).

$$\frac{ABS}{RC} = \frac{M_0}{V_J} \times \frac{F_M - F_0}{F_M} \tag{12}$$

Statistical analysis

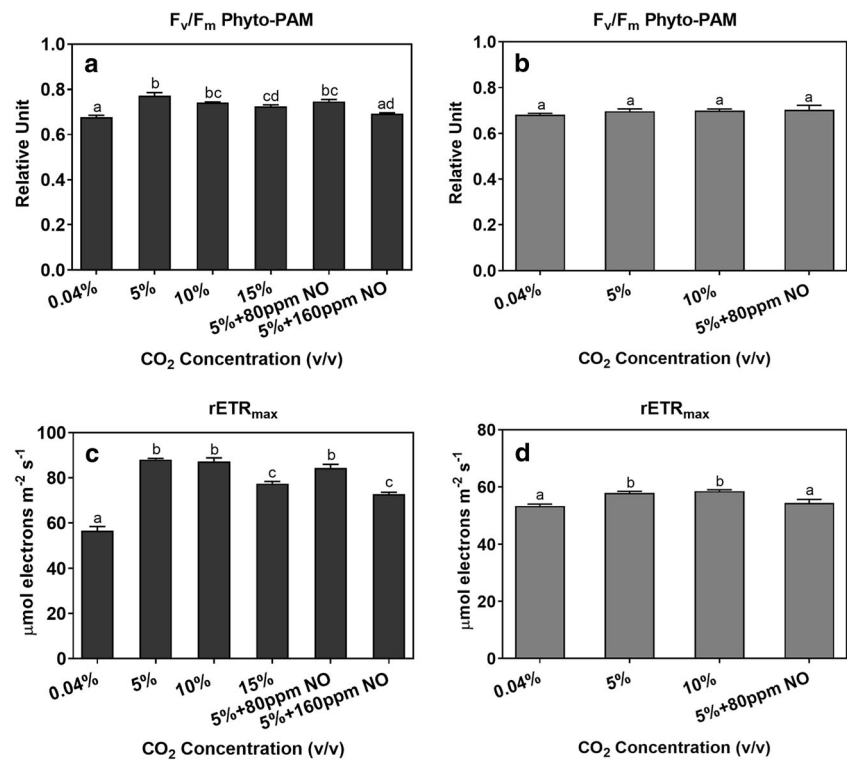
Comparison of parameters (obtained during log phase) with respect to changing gas concentrations was tested by one-way ANOVA, which was then followed by a Tukey multiple-comparison test. Parameters involving the additional variable of changing growth phase were compared by using two-way RM ANOVA, which was followed by a Sidak multiple-comparison test. All the analyses were carried out by using the statistical software GraphPad Prism version 7.02 for Windows, GraphPad Software, USA, www.graphpad.com. A P value ≤ 0.05 was considered statistically significant.

Results

RLC measurements

We find the F_v/F_m values for both the species to be in the range of 0.68–0.77 under the conditions tested (Fig. 1a, b). The high- CO_2 -grown cells of *C. sorokiniana* exhibited higher yields of PSII than the ambient-grown cells with the highest F_v/F_m of 0.77 under 5% CO_2 . The F_v/F_m values did not change significantly between 5% and 10% CO_2 and 5% CO_2 + 80 ppm NO-grown cells. Whereas, the F_v/F_m values of the 15% CO_2 and 5% CO_2 + 160 ppm NO-grown cells were found to be lower than that of 5% CO_2 -grown cells. On the other hand, the F_v/F_m values of *A. quadricellulare* remained unchanged at around 0.70 under all the conditions tested. Further, similar to the pattern observed for F_v/F_m , the $rETR_{max}$ of *C. sorokiniana* appeared to be more responsive to CO_2 concentration than *A. quadricellulare*. When the CO_2 level for growth was increased from 0.04 to 5% v/v, the $rETR_{max}$ in the former species increased by 55.8%, while in the latter it only increased by 8.6% (Fig. 1c, d). For both the species, the maximum $rETR_{max}$ was attained at 5% CO_2 , and

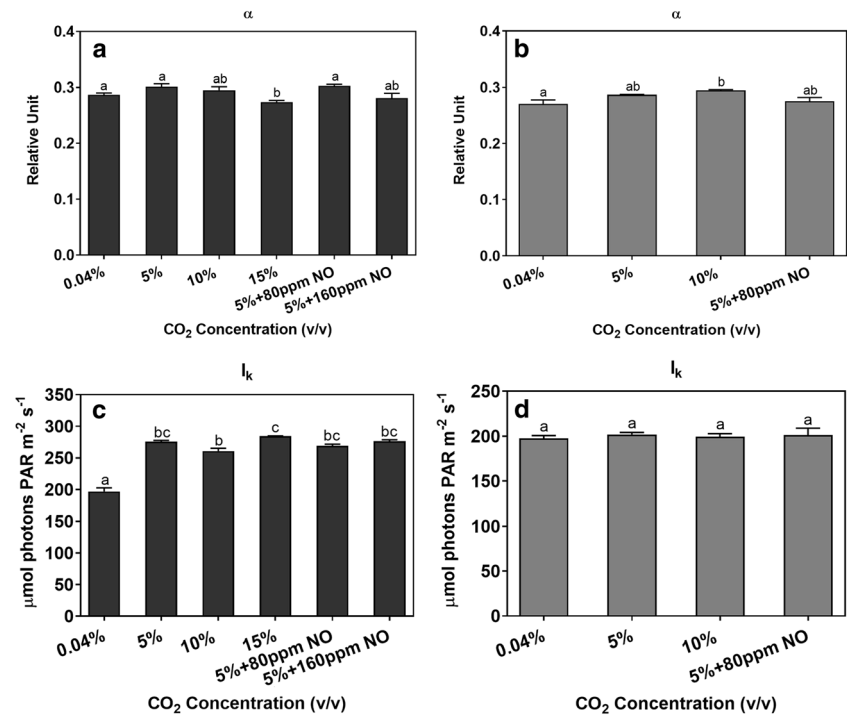
Fig. 1 Effect of CO₂ and NO levels on the **a, b** maximum quantum yield of PSII (F_v/F_m); and **c, d** maximum relative electron transport rate ($rETR_{max}$) of *C. sorokiniana* and *A. quadricellulare*, respectively. Experiments were conducted in a semi-continuous culture mode at 37 °C and 14:10 LD cycle that had a light regime of 14 h sine function at an amplitude of 250 $\mu\text{mol photons m}^{-2} \text{s}^{-1}$. Air that contained specific concentrations of CO₂ and NO was bubbled through the cultivation vessels at an aeration rate of 0.45 vvm. The bars that are marked with different letters are significantly different ($P < 0.05$). (Data are shown as mean \pm SEM, $n = 3$)



no significant difference was observed between the $rETR_{max}$ of 5% and 10% CO₂ cultivated cells. In *C. sorokiniana*, the $rETR_{max}$ declined as the CO₂ level was raised from 10 to 15%; however, blending 80 ppm NO with 5% CO₂ did not affect this parameter, and it remained in the range of 5% and 10% CO₂ cultivated cells. A further increment in NO from 80 to

160 ppm led to a decline in $rETR_{max}$ to the level of 15% CO₂ cultivated cells. In the case of *A. quadricellulare*, although F_v/F_m remained unaffected, a marginal decline of 7% in $rETR_{max}$ was observed when cells that were grown under 10% CO₂ were compared with cells that were cultivated at 5% CO₂ + 80 ppm NO gas concentration.

Fig. 2 Effect of CO₂ and NO levels on the **a, b** light harvesting efficiency (α) and **c, d** light saturation parameter (I_k) of *C. sorokiniana* and *A. quadricellulare*, respectively. Refer to the legend to Fig. 1 for additional details. Since we did not measure true ETR, α values are only relative



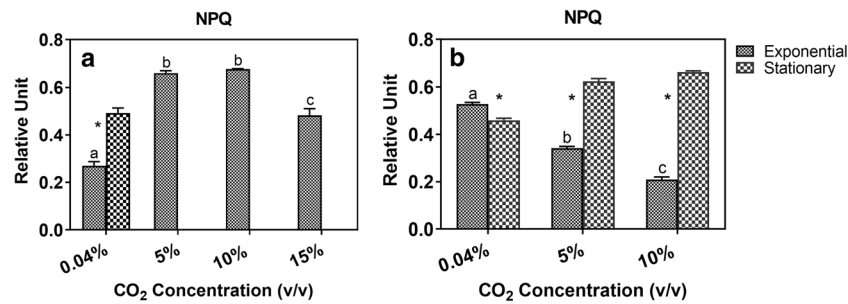


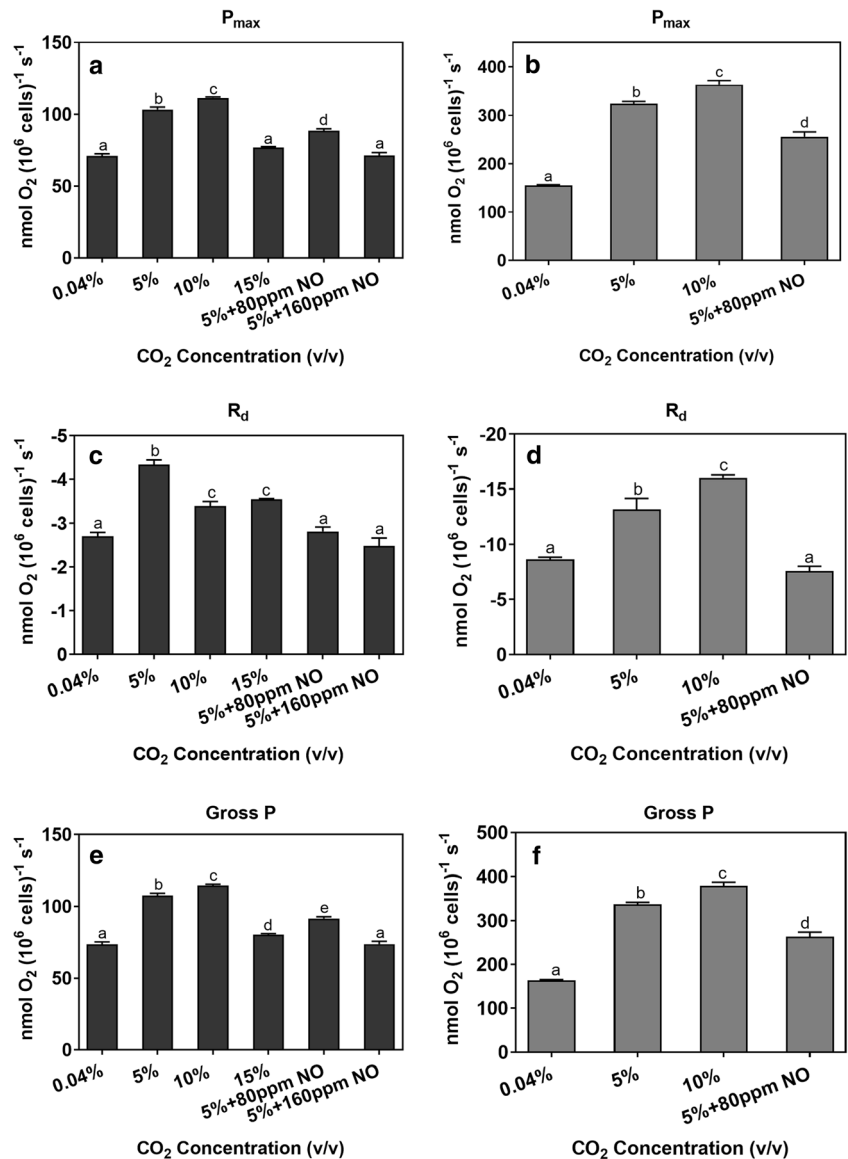
Fig. 3 Effect of CO₂ levels on the NPQ capacity of **a** *C. sorokiniana* and **b** *A. quadricellulare*, respectively. The bars that are marked with different letters are significantly different. The asterisks indicate significant

differences between the log and stationary phases of cells at each gas concentration ($P < 0.05$). Refer to the legend of Fig. 1 for additional details

For *C. sorokiniana*, the value of α remained unchanged up to 10% CO₂ but declined marginally at 15% CO₂. However, in *A. quadricellulare*, the α value at 10% CO₂ was slightly higher than that observed at ambient CO₂ but was in the range of α values at 5% CO₂ and

5% CO₂ + 80 ppm NO (Fig. 2a, b). In *C. sorokiniana*, a higher I_k was observed under elevated CO₂ concentrations than at ambient conditions and I_k in *A. quadricellulare* remained constant across all the tested gas levels (Fig. 2c, d).

Fig. 4 Effect of CO₂ and NO levels on the **a, b** maximum photosynthetic rates (P_{max}), **c, d** dark respiration rates (R_d), and **e, f** gross photosynthetic rates (Gross P) of *C. sorokiniana* and *A. quadricellulare*, respectively. Refer to the legend of Fig. 1 for additional details



NPQ analysis

In the exponential growth phase, ambient-grown cells of *C. sorokiniana* had the lowest NPQ capacity, which increased as the CO₂ concentration was raised to 5% v/v. No significant difference between the NPQ capacity of 5% and 10% CO₂-grown cells was noted. However, the NPQ declined as the CO₂ level was further increased to 15% v/v. During the stationary phase, the ambient-grown cells showed an increase in NPQ, while the cells that were cultivated under high-CO₂ levels exhibited negligible NPQ (Fig. 3a). In the case of *A. quadricellulare*, during the log phase, the ambient-grown cells exhibited maximum NPQ capacity, and NPQ declined with increasing CO₂ concentration. However, except for the ambient condition, NPQ increased as the cells moved from log to stationary phase (Fig. 3b).

Overall, the photosynthetic parameters that were obtained from the Phyto-PAM measurements reveal that *C. sorokiniana* was more responsive to changing gas concentrations and had a higher tolerance to CO₂ and NO than *A. quadricellulare*.

Dark respiration and photosynthesis

Both P_{\max} and R_d were stimulated under elevated levels of CO₂ compared to values under ambient conditions. The saturating light intensity that was used to obtain P_{\max} was 505 and 435 $\mu\text{mol photons m}^{-2} \text{s}^{-1}$ for *C. sorokiniana* and *A. quadricellulare*, respectively. In general, the magnitudes of P_{\max} and R_d of *A. quadricellulare* were always higher than those of *C. sorokiniana*. For both species, P_{\max} increased linearly from ambient to 10% CO₂ concentration. Further, in *C. sorokiniana*, P_{\max} declined by ~31% as the CO₂ concentration

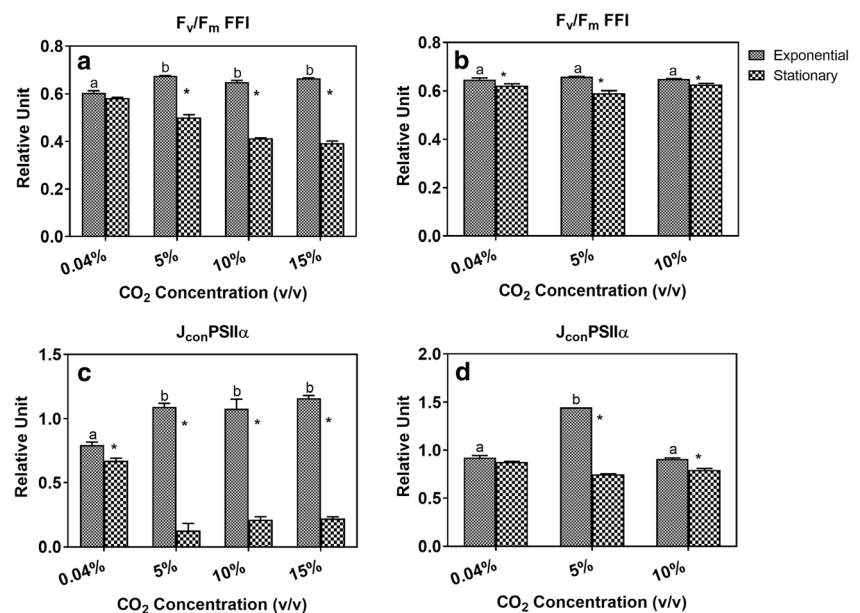
increased from 10 to 15% v/v. For both species, NO-supplemented cells exhibited lower P_{\max} values than those obtained for cells that were cultivated in mixtures of only air + CO₂ (Fig. 4a, b).

We observed that *C. sorokiniana* exhibited the highest R_d at 5% CO₂-level, and this declined as the CO₂ concentration for growth was increased further to 10% v/v. No significant difference between the R_d of 10% and 15% CO₂-grown cells was observed; however, R_d declined further when CO₂ was blended with NO. On the other hand, in *A. quadricellulare*, R_d followed the same pattern as that of P_{\max} (Fig. 4c, d).

FFI curve analysis

The F_v/F_m values obtained from the FFI technique exhibited a pattern that was similar to the values that were obtained from the PAM-RLCs. The stationary phase measurements of FFI curves show that F_v/F_m declined as the cultures moved from the exponential to the stationary phase (Fig. 5a, b). The antenna connectivity parameter $J_{\text{con}}\text{PSII}\alpha$ is dependent on both the connectivity of photosynthetic units as well as the reaction center parameters. In both the species, the $J_{\text{con}}\text{PSII}\alpha$ was higher during the log phase than that was observed during the stationary phase. Moreover, in *C. sorokiniana*, the $J_{\text{con}}\text{PSII}\alpha$ of elevated-CO₂-grown cells was higher than that of ambient-grown cells, and a good correlation was observed between the antenna connectivity and NPQ. On the contrary, despite the lower NPQ capacity of 5% CO₂-grown cells of *A. quadricellulare*, their $J_{\text{con}}\text{PSII}\alpha$ was higher than that of ambient and 10% CO₂-grown cells, which represent a weaker correlation between $J_{\text{con}}\text{PSII}\alpha$ and NPQ (Fig. 5c, d).

Fig. 5 Effect of CO₂ concentration and the changing growth stage on the **a, b** maximum quantum yield of PSII (F_v/F_m) and **c, d** antenna connectivity parameter of PSII α ($J_{\text{con}}\text{PSII}\alpha$) of *C. sorokiniana* and *A. quadricellulare*, respectively. The statistical representation is as described in the legend to Fig. 3. Refer to the legend of Fig. 1 for additional details



During the log phase, there was no alteration in the antenna heterogeneity, whereas during the stationary phase elevated CO₂ grown cells exhibited a higher percentage of PSII α and a lower percentage of PSII β than that which was seen in ambient-grown cells. Thus, overall, as the cells moved from the exponential to stationary phase, there was a significant rise in the percentage of PSII α centers and a drop in the percentage of PSII β centers of high-CO₂-grown cells while the heterogeneity remained unaltered in ambient-grown cells (Fig. 6a–d).

In *C. sorokiniana*, the log phase σ PSII α of ambient-grown cells was marginally higher than that of high-CO₂-grown cells. As the cells moved to stationary phase, a remarkable increase in the values of σ PSII α was observed; however, this increment was more pronounced under high CO₂ than under an ambient condition (Fig. 7a). On the contrary, in *A. quadricellulare*, the log phase value of σ PSII α remained unchanged under all the tested levels of CO₂, and no significant change was observed even when the cells progressed to the stationary phase (Fig. 7b). Further, in *C. sorokiniana*, varying CO₂ concentration did not have any significant effect on the log phase values of σ PSII β (Fig. 7c). However, the log phase values of σ PSII β in *A. quadricellulare* were higher for elevated CO₂-grown cells than for ambient-grown cells. Though an increase in the σ PSII β value of ambient-grown cells was observed with the changing growth stage, this parameter remained unchanged in high-CO₂-grown cells (Fig. 7d).

OJIP transients

Fluorescence induction (FI) curves of *A. quadricellulare* cells that were cultivated under ambient air showed lower overall fluorescence intensity than those that were cultivated under

high-CO₂ (Fig. 8a). On the contrary, for *C. sorokiniana*, the fluorescence intensity remained unaltered up to 10% CO₂; however, significant changes were observed as the CO₂ level was raised to 15% v/v (Fig. 8b). Furthermore, despite the decline in the fluorescence intensity, the shape of the OJIP curve was not greatly affected. Based on these fluorescence signals, selected parameters were calculated for *A. quadricellulare* and *C. sorokiniana* (Tables 1 and 2, respectively).

In *C. sorokiniana*, the elevated concentrations of CO₂ led to lower values of V_J than those that were obtained under an ambient CO₂ level. However, in the case of *A. quadricellulare*, the value of V_J remained unchanged under all tested CO₂ levels. Further, in *C. sorokiniana*, the ϕ_{P0} of ambient-grown cells was lower than that of cells that were cultivated under elevated CO₂. However, no significant difference between the ϕ_{P0} values of 5%, 10%, and 15% of CO₂-grown cells was observed. On the other hand, in *A. quadricellulare*, ϕ_{P0} remained unchanged under all the tested CO₂ levels. These results agree well with the F_v/F_m values that were obtained from FFI measurements. A similar pattern was also obtained for the yield of electron movement into the ETC per trapped exciton (Ψ_0) (Tables 1 and 2).

In *C. sorokiniana*, the absorption flux per reaction center (ABS/RC) of ambient-grown cells was more than that of 5% and 15% CO₂-grown cells even though the Chl *a* content of the former was lower than that of the latter (Table 1, Supplementary information). Also, despite having a smaller antenna size than those of ambient and 10% CO₂-treated cells, the highest Chl *a* content of 5% CO₂-grown cells indicates that the largest number of active RCs occur at this gas concentration. Similarly, regardless of the lower Chl *a* content in 10% CO₂-grown cells (Table 2, Supplementary information),

Fig. 6 Effect of CO₂ levels and the changing growth stage on the **a, b** proportion of α centers of PSII, PSII α and **c, d** proportion of β centers of PSII, PSII β of *C. sorokiniana* and *A. quadricellulare*, respectively. The statistical representation is as described in the legend to Fig. 3. Refer to legend of Fig. 1 for additional details

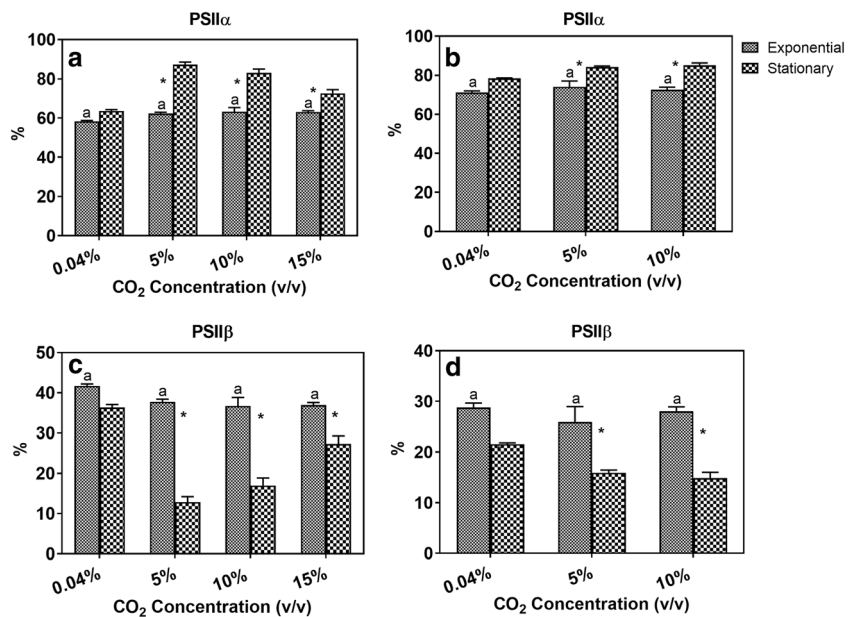
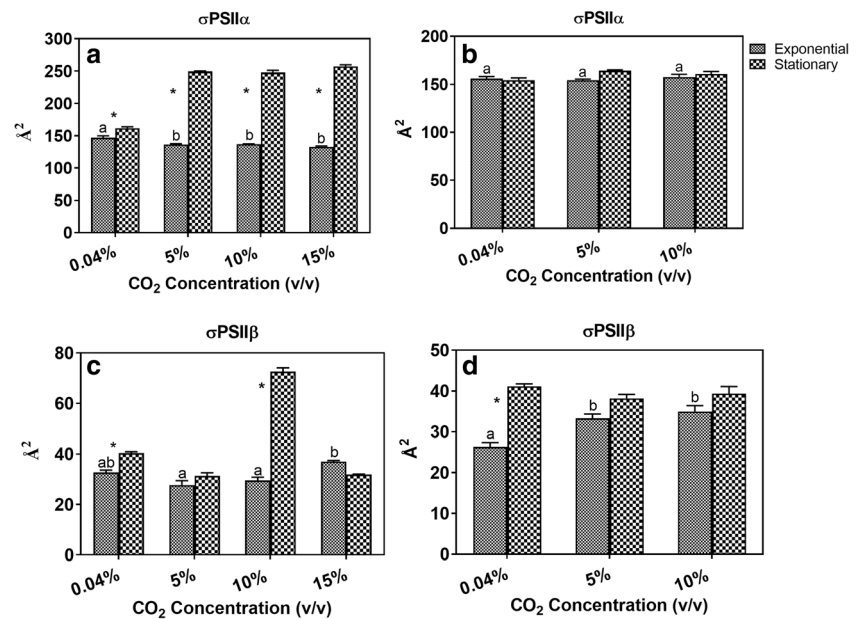


Fig. 7 Effect of CO₂ levels and the changing growth stage on the **a, b** effective absorption cross-sectional area of PSII α centers, σ PSII α and **c, d** effective absorption cross-sectional area of PSII β centers, σ PSII β of *C. sorokiniana* and *A. quadricellulare*, respectively. The statistical representation is as described in the legend to Fig. 3. Refer to the legend of Fig. 1 for additional details



the comparable ABS/RC of ambient and 10% CO₂-grown cells in *A. quadricellulare* is an indicator of the presence of a larger number of inactive PSII centers at 10% CO₂. Since we could not find any specific pattern in other flux values such as trapping flux (TR_o/RC), electron transport flux (ET_o/RC), and dissipated energy flux (DI_o/RC), they have not been discussed further here.

The JIP analysis shows that the performance index on absorption basis (PI_{ABS}) of the high CO₂-grown cells of *C. sorokiniana* was significantly higher than that of the ambient-grown cells, and the PI_{ABS} values of 5%, 10%, and 15% CO₂-grown cells were comparable to each other. This is in agreement with the F_v/F_m values that were obtained from FFI measurements. In contrast, in *A. quadricellulare*, even though F_v/F_m remained unchanged under different CO₂ levels, PI_{ABS} went up when the CO₂ concentration was increased from ambient to 5% but decreased at 10% CO₂.

Similar to the sigmoidicity parameter J (obtained from the FFI measurements), a few other parameters such as the C_{HYP} and p_{2G} , obtained from OJIP transients, are typically used to compare the connectivity between the PSII units. In *C. sorokiniana*, growth under 5% and 10% CO₂ led to better energetic connectivity (higher C_{HYP} and p_{2G}) between the

PSII units than that was observed under ambient conditions. However, further increase in CO₂ levels to 15% v/v significantly reduced the connectivity between the PSII units and the numerical values of C_{HYP} and p_{2G} were even smaller than those that were obtained under ambient conditions. Likewise, in *A. quadricellulare*, 5% CO₂-grown cells exhibited better energetic connectivity between the PSII units over ambient cells, while 10% of CO₂ grown cells exhibited the lowest connectivity among all the three CO₂ treatments.

Discussion

Our results show that statistically significant differences in the performance and composition of the photosynthetic physiology of *C. sorokiniana* and *A. quadricellulare* were observed under elevated concentrations of CO₂ and NO. The F_v/F_m is often used as a sensitive indicator of stress in organisms that perform oxygenic photosynthesis. For healthy and non-stressed cells, this value is approximately 0.83 for most vascular plants, and between 0.6 and 0.65 for green algae; the yield declines as stress to PSII increases (Maxwell and Johnson 2000; Dao and Beardall 2016b). The PAM results show that under the tested

Fig. 8 OJIP transients of cells of **a** *A. quadricellulare* and **b** *C. sorokiniana* cultivated under different CO₂ concentrations. Refer to the legend of Fig. 1 for details on operating conditions

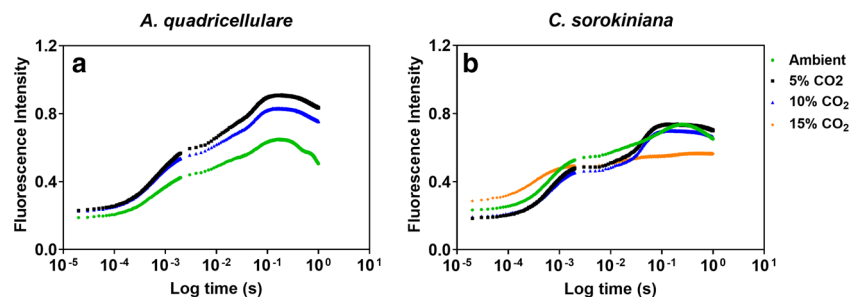


Table 1 PSII photophysiological parameters of *A. quadricellulare* under CO₂ treatments, determined from the OJIP transients (± SEM) and calculated according to the equations discussed above

	Ambient (0.04%)	5%	10%
V _J (2 ms)	0.495 ± 0.010 ^a	0.487 ± 0.002 ^a	0.517 ± 0.012 ^a
M ₀	0.515 ± 0.014 ^a	0.477 ± 0.009 ^a	0.571 ± 0.002 ^b
φ _{PO} = F _v /F _m	0.759 ± 0.006 ^a	0.773 ± 0.001 ^a	0.771 ± 0.003 ^a
Ψ ₀	0.505 ± 0.010 ^a	0.512 ± 0.002 ^a	0.483 ± 0.012 ^a
ABS/RC	1.369 ± 0.006 ^a	1.267 ± 0.026 ^b	1.435 ± 0.028 ^a
PI _{ABS}	2.352 ± 0.112 ^a	2.835 ± 0.077 ^b	2.202 ± 0.099 ^a
C _{HYP}	1.054 ± 0.076 ^a	1.929 ± 0.145 ^b	0.514 ± 0.020 ^c
P _{2G}	0.335 ± 0.023 ^a	0.566 ± 0.039 ^b	0.153 ± 0.008 ^c

Significant differences are indicated by different letters (a, b, and c). *A. quadricellulare* did not grow under 15% CO₂; therefore, there is no data for that condition

gas levels, the F_v/F_m values of both the species were within the range for healthy green algae, which implies that the tested concentrations of CO₂ and NO did not cause any stress to the overall functioning of PSII. The lower F_v/F_m that was obtained for ambient-grown cells of *C. sorokiniana* could be due to an increase in the backward flow of electrons from Q_A⁻ to the water side in PSII. This reduces the normal transport of electrons from PSII to PSI, which leads to a reduction in the apparent concentration of reduced Q_A, thus resulting in a lower fluorescence yield. A similar phenomenon has been reported previously when air-adapted cells of *Chlamydomonas reinhardtii* exhibited lower fluorescence yield than high CO₂-cultivated cells (Mende 1980; Spalding et al. 1984). Further, the rETR is a measure of the number of electrons that pass through PSII per unit time; therefore, rETR_{max} can be used to estimate the capacity of the photosynthetic apparatus at saturating light (Ralph and Gademann 2005). The rETR_{max} of high CO₂ grown cells was higher than that of ambient-grown cells. Reports in the literature suggest that under current levels of CO₂ (~ 400 ppm), photosynthesis, in higher plants at least, can be limited by the activity of ribulose-1,5-bisphosphate carboxylase/oxygenase (RuBisCo) (Bernacchi et al. 2005; Ainsworth and Rogers 2007). While microalgae possess CCMs to improve

Rubisco carboxylation efficiency (Giordano et al. 2005), these will be repressed under the elevated CO₂ concentrations used here. As the concentration of CO₂ rises, the carbon fixation rate increases, which implies that the demand for ATP that is required for the regeneration of ribulose-1,5-bisphosphate (RuBP) also goes up. As a result, the control of photosynthesis shifts from RuBisCo to RuBP regeneration, and resource investment from carboxylation to electron transport takes place, which results in higher rETR_{max} at elevated levels of CO₂ (Bernacchi et al. 2005; Ainsworth and Rogers 2007; Li et al. 2015). Under enhanced electron transport, the stimulated photosynthetic uptake of CO₂ also led to improved growth rates (Varshney et al. 2018). Simulated growth rates have also been observed in a number of previous studies (Qiu and Gao 2002; Yang and Gao 2003). The parameter α is a function of both the light harvesting efficiency and the photosynthetic energy conversion efficiency (Henley 1993). Previous studies have also correlated changes in α with the changes in cell pigment composition or content and the associated proteins that are present in the light-harvesting complex (LHCs) (Pierangelini et al. 2014a; Kamalanathan et al. 2016), both of which can be affected by CO₂. In *C. sorokiniana*, the lower value of α at 15% CO₂ (compared to 5% CO₂) can be correlated to the lower pigment content/cell at this CO₂ level, which would further indicate a lower light harvesting ability at this gas concentration. However, in both the species, though the chlorophyll content was lower at 10% CO₂, α at this CO₂ level was comparable with values obtained for cells grown at 5% CO₂ and 5% CO₂ + 80 ppm NO, which suggests that the algae had alternate ways to compensate for the lower chlorophyll values up to 10% v/v CO₂ (Table 1 and 2, Supplementary information). This result is in line with previous reports (Dao and Beardall 2016a). I_k is commonly used to compare the photoacclimation status of algae, both between as well as within species (Henley 1993). For *C. sorokiniana*, the higher I_k observed under elevated CO₂ concentrations when compared to ambient-grown condition could be correlated to simulated photosynthetic capacity (rETR) of cells under high CO₂. In contrast, the constant I_k for *A. quadricellulare* under all the tested gas levels imply that the ratio of rETR_{max} and α remained the same, despite the

Table 2 PSII photophysiological parameters of *C. sorokiniana* under CO₂ treatments, determined from the OJIP transients (± SEM) and calculated according to the equations discussed above

	Ambient (0.04%)	5%	10%	15%
V _J (2 ms)	0.561 ± 0.002 ^a	0.521 ± 0.006 ^b	0.50 ± 0.008 ^b	0.519 ± 0.002 ^b
M ₀	0.574 ± 0.005 ^a	0.518 ± 0.012 ^b	0.529 ± 0.014 ^{ab}	0.483 ± 0.008 ^b
φ _{PO} = F _v /F _m	0.728 ± 0.007 ^a	0.786 ± 0.007 ^b	0.777 ± 0.002 ^b	0.779 ± 0.003 ^b
Ψ ₀	0.439 ± 0.003 ^a	0.479 ± 0.006 ^b	0.50 ± 0.008 ^b	0.481 ± 0.002 ^b
ABS/RC	1.404 ± 0.012 ^a	1.259 ± 0.020 ^b	1.361 ± 0.018 ^a	1.169 ± 0.011 ^c
PI _{ABS}	1.49 ± 0.018 ^a	2.73 ± 0.14 ^b	2.569 ± 0.14 ^b	2.803 ± 0.070 ^b
C _{HYP}	0.829 ± 0.05 ^a	1.676 ± 0.002 ^b	1.463 ± 0.07 ^b	0.132 ± 0.004 ^c
P _{2G}	0.31 ± 0.017 ^a	0.449 ± 0.007 ^b	0.42 ± 0.02 ^b	0.038 ± 0.002 ^c

Significant differences are indicated by different letters (a, b, and c)

fluctuations in their individual values. Similar effects were also reported, for example, in the red macroalga *Palmaria palmata* and the cyanobacterium *Cylindrospermopsis raciborskii*, where the former did not show a significant increase in I_k , but the latter showed an enhanced I_k value under elevated CO_2 levels (Pierangelini et al. 2014b; Sebök et al. 2017).

NPQ is a mechanism of regulating and protecting the photosynthetic apparatus when the absorption of light energy exceeds its utilization (Müller et al. 2001). The NPQ capacity of *C. sorokiniana* increased in going from ambient to 5% CO_2 level. Iwasaki et al. (1996) also reported a marginal increase in the NPQ capacity of the marine green microalga *Chlorococcum littorale*, when its cells were shifted from ambient to a high- CO_2 level (40% v/v). However, these researchers could not provide a rationalization for this change (Iwasaki et al. 1996). It is evident that under CO_2 -limited conditions (ambient-grown cells), the CCM is activated, which increases the uptake of inorganic carbon (C_i) into the cell, due to which the photosynthetic CO_2 -utilization efficiency also increases. However, the CCM is a highly energy-intensive process (Raven et al. 2014), and this could be a mechanism adopted by ambient-grown cells to dissipate excess excitation energy (Tchernov et al. 1998). In contrast, high- CO_2 -grown cells do not express CCMs; thus, an alternative dissipation process, NPQ, is used. Further, the lower value of NPQ at the 15% CO_2 level might reflect the reduced performance of photoprotective mechanisms under this condition, which may lead to photodamage. Alternatively, *A. quadricellulare* exhibited maximum NPQ capacity under ambient conditions. It has been reported that during CCM induction, organisms shift their photosynthetic linear ETC to cyclic electron transport flow around PSI by means of a state transition (Falk and Palmqvist 1992; Pierangelini et al. 2014b). This satisfies the higher ATP requirements for active C_i transport. However, if energy dissipation via CCM activity and C assimilation is inadequate, then cells need to engage NPQ, as appears to be happening with the log phase cells of *A. quadricellulare*. Further, suppression of CCMs (under high CO_2) results in high NADPH requirements, which stimulate NADP^+ reduction by linear electron transport. Hence, NPQ decreases as the CO_2 level goes up. A similar phenomenon has also been reported by Li et al. (2016), in which ambient-grown cells of *C. sorokiniana* exhibited greater NPQ capacity than 1% CO_2 -grown cells. Likewise, Sebök et al. (2017) also reported that in the red macroalga *P. palmata*, the need for energy dissipation via NPQ declined as the CO_2 levels increased.

The higher magnitudes of P_{max} and R_d for *A. quadricellulare* than those for *C. sorokiniana* could be due to bigger cells of the former than those of latter. The details on the growth rates (μ_{max}) and cell size of these species have been provided previously (Varshney et al. 2018). In *C. sorokiniana*, despite the comparable μ_{max} and rETR_{max} of

5% and 10% CO_2 -grown cells, the P_{max} of the latter was marginally higher than that of the former. This indicates that along with the downregulation of CCM, the increase in CO_2 concentration also enhanced the capacity of cells to carry out light-saturated photosynthesis and incorporate carbon into carbohydrates (Pierangelini et al. 2014b; Varshney et al. 2018). A further increment in CO_2 level from 10 to 15% led to a decline in P_{max} , which was also supported by the lower μ_{max} , rETR_{max} , and the smaller cell size of the latter as reported previously (Varshney et al. 2018). Likewise, the lower P_{max} of NO -supplemented cells can also be attributed to the smaller biovolume of these cells (Varshney et al. 2018).

In the present study, a decrease in F_v/F_m was observed when the culture moved from log to stationary phase. Previous reports suggest that this could be an indicator of PSII impairment and can be attributed to either a decline in the proportion of PSII RCs that are capable of performing photochemistry and/or an increase in NPQ (Maxwell and Johnson 2000; Dao and Beardall 2016a). In our case, under elevated CO_2 , a decline in the stationary phase F_v/F_m values of *A. quadricellulare* can be correlated to both the increased inactive RCs as well as to the increased NPQ. However, in *C. sorokiniana*, except for ambient-grown cells that did not show any difference between the log and stationary phase values of F_v/F_m , a decline in the stationary phase values obtained at all other gas levels can be attributed only to increased inactive RCs as NPQ was negligible during the stationary phase. Further, $J_{\text{con}}\text{PSII}\alpha$ describes the migration of excitation energy from closed to open PSII centers and the extent to which the PSII antenna can be described as a lake where PSII centers are energetically connected by a shared antenna, as opposed to an isolated unit where each PSII reaction center only receives energy from its neighboring antenna (Lavergne and Trissl 1995). The higher values of $J_{\text{con}}\text{PSII}\alpha$ observed for high- CO_2 -grown cells support the lake model and confirms the presence of more energetically connected antennae than that was observed for ambient grown cells. In addition, log phase cells exhibited better connectivity between RCs than the stationary phase cells.

It has been reported that the antenna heterogeneity varies both with alteration in growth conditions as well as in growth stage (Marchin et al. 2014). Further, the $\text{PSII}\alpha$ centers are distinguished from $\text{PSII}\beta$ centers by their bigger antenna size (2–3 times bigger than that of $\text{PSII}\beta$), higher degree of excitation transfer between themselves and the plastoquinone pool (high degree of connectivity), and their inability in the transferring of energy to PSI (Marchin et al. 2014; Pierangelini et al. 2014b). Previous reports suggest that under CO_2 -enriched conditions when the CCM is downregulated, a higher percentage of $\text{PSII}\alpha$ centers and a lower percentage of $\text{PSII}\beta$ centers are attained in comparison to the proportions that are attained under CO_2 -limited conditions (Pierangelini et al. 2014b). Also, when the cells are stressed, the number

of inactive RCs rises, and the contribution of PSII β centers and Q_B non-reducing centers goes up (Markou et al. 2017). However, in the present study, a decline in PSII β reaction centers during the stationary phase could be correlated to a transition from state 2 to state 1, which leads to conversion of PSII β to PSII α and either of PSII α or PSII β can be active or inactive (Pierangelini et al. 2014b; Dao and Beardall 2016a).

Further, one of the fundamental properties that are responsible for the efficient functioning of the photosynthetic light-harvesting antenna (open PSII units) is its functional absorption cross-sectional area (σ_{PSII}), which is expressed in terms of area (\AA^2) (Ihnken et al. 2011; Ruban et al. 2011). It defines the size of the antenna pigments transferring excitation to the functional PSII RC and therefore, the rate at which photons are delivered to PSII RCs for a given photon flux to the antenna (Cosgrove and Borowitzka 2010). Similar to the present study, Pierangelini et al. also reported that the $\sigma_{\text{PSII}\alpha}$ of high- CO_2 -cultivated cells of *C. raciborskii* CS506 was lower than that of low- CO_2 -cultivated cells (Pierangelini et al. 2014b). The smaller antenna size can increase the photon use efficiency of algae as it minimizes the wasteful dissipation of absorbed light energy and allows better light penetration (Melis et al. 1998; Seth and Wangikar 2015). This could be the cause of higher light-saturated photosynthetic rates (P_{max}) under high- CO_2 levels. In contrast, a significant increase in the antenna size during the stationary phase could be a way to compensate for the damage (lower F_v/F_m in the stationary phase, see Fig. 5a) that is caused by prolonged exposure to such high concentrations of CO_2 .

A number of reports suggest that when the algal cells are cultivated under stress conditions such as high temperature (Zhao et al. 2008), high salt concentration (Zhang et al. 2010b), high metal concentration (Zhang et al. 2010a), and ammonia toxicity (Markou et al. 2016), the F_m value decreases and the shape of the FI curve becomes almost flat. This decrease in F_m and fluorescence levels can be attributed to the inhibition of electron transport after Q_A , and the inability of the OEC to provide electrons to PSII and to reduce PQ (Strasser and Srivastava 1995; Markou et al. 2017). In the present study, despite the decline in the fluorescence intensity, the relatively unaltered shape of the OJIP curve suggests that the growth inhibition was not severe. Among the calculated parameters, V_j is used as an estimation of Q_B non-reducing RCs, that is, the number of reaction centers that cannot transfer electrons from Q_A to Q_B (Jianrong and Qiran 2009; Markou et al. 2016). In the case of *C. sorokiniana*, the lower values of V_j under elevated concentrations of CO_2 indicate the stronger limitation of electron transfer from Q_A to Q_B under ambient conditions. However, the constant value of V_j for *A. quadricellulare* under all the tested CO_2 levels implies that the capacity for reoxidation of Q_A^- remained unaltered with changing CO_2 concentrations. The higher ABS/RC of

ambient-grown cells than that of 5% and 15% CO_2 -grown cells could be correlated to either the presence of a larger number of inactive PSII centers or an increase in the accumulation of PSII β centers. In our case, the accumulation of PSII β did not change with changing concentrations of CO_2 (from results of FFI analysis); therefore, the observed higher ABS/RC is likely to be associated with an increase in the inactive PSII centers. In addition, the highest Chl *a* content of 5% CO_2 -grown cells indicate the presence of the largest number of active RCs that occur at this gas concentration. The parameter, ABS/RC, represents the incident photon flux that was absorbed by the antenna pigments, thus forming the excited chlorophyll, Chl* (Strasser et al. 2004; Dao and Beardall 2016a). Similarly, regardless of the lower Chl *a* content in 10% CO_2 -grown cells, the comparable ABS/RC of ambient and 10% CO_2 -grown cells in *A. quadricellulare* is an indicator of the presence of larger number of inactive PSII centers at 10% CO_2 . As evident from Eq. 9, the PI_{ABS} combines three different functional steps of photosynthesis such as the (i) absorption of light energy, (ii) trapping of excitation energy, and (iii) conversion of trapped energy to electron transport, into one parameter and computes the PSII photosynthetic activity (Kalaji et al. 2014; Dao and Beardall 2016a). The PI_{ABS} of *C. sorokiniana*, obtained from OJIP analysis, was consistent with the F_v/F_m obtained from FFI measurements. However, in *A. quadricellulare*, despite the constant F_v/F_m for all the tested CO_2 levels, the overall photosynthetic activity of 5% of CO_2 grown cells was more than that of ambient-grown cells. This is because the PI_{ABS} is a more sensitive indicator of stress in photosynthesis than F_v/F_m alone and the effect of varying concentrations of CO_2 on the other steps, which have been discussed in “OJIP transients” section, was more profound than that on the primary photochemistry alone.

Other parameters such as p_{2G} and C_{HYP} which have been recommended for evaluating the connectivity between the PSII units, were also derived from the OJIP transients. The lower values of p_{2G} and C_{HYP} signify lower connectivity between PSII units, which also implies that only a smaller fraction of excitation energy is used for photochemistry and the larger portion is dissipated as heat and fluorescence. On the contrary, higher p_{2G} and C_{HYP} reflect the clear sigmoidal shape of the fluorescence transient and higher energetic connectivity between the PSII units. Although it has been reported previously that a decline in connectivity between PSII centers is correlated with the decrease in the percentage of PSII α centers (Kyle et al. 1982), we did not observe any change in the proportion of PSII α centers with changing connectivity.

Overall, although there was a drastic effect on the photosynthetic apparatus and performance of *C. sorokiniana* at 15% CO_2 , *A. quadricellulare* showed almost consistent performance across all tested CO_2 concentrations.

Conclusion

This study demonstrated the long-term (spanning several weeks) effect of elevated levels of CO₂ and NO, which are typically present in the industrial flue gases, on the photosynthetic mechanism of two freshwater green microalgal isolates. Under different gas concentrations, the photosynthetic regulatory patterns in the selected species were significantly different from each other. However, both the species maintained their photosynthetic capacity by using simple, low biological cost mechanisms of antenna size and changes in the proportion of PSII centres, in parallel with the alterations in the energetic connectivity between PSII units. The photosynthetic efficiency for carbon acquisition was significantly higher at elevated CO₂ levels than that was observed under ambient conditions. The optimal CO₂ concentration for both the species was 5% v/v; however, the photosynthetic apparatus was not under much stress up to a CO₂ level of even 10% v/v. Moreover, the blending of NO (with CO₂ and air) up to the tested levels did not have any severe impact on the quantum yield and photosynthetic capacity of algal cells. Although, the photosynthetic performance observed under laboratory conditions cannot fully predict the behavior of algae in the field because diurnal changes in the solar photon flux density, cloud cover, temperature cues, and vertical migrations are just a few of the other factors that also induce considerable changes in the photochemical properties of algae. Nonetheless, this bench-scale study on the selected novel algal species is the first of many steps that ensures that the selected candidates are suitable for further investigations in large-scale photobioreactors and ponds for CO₂ and NO mitigation from flue gases.

Acknowledgments This work was supported by the JSW Foundation, India, Wadhvani Research Centre for Bioengineering, IIT Bombay, India and the Department of Biotechnology, Ministry of Science and Technology, Government of India (Grant No: BT/EB/PAN IIT/2012).

Compliance with ethical standards

Conflict of interest The authors declare that they have no conflict of interest.

References

- Ainsworth EA, Rogers A (2007) The response of photosynthesis and stomatal conductance to rising [CO₂]: mechanisms and environmental interactions. *Plant Cell Environ* 30:258–270
- Antal T, Rubin A (2008) In vivo analysis of chlorophyll *a* fluorescence induction. *Photosynth Res* 96:217–226
- Baker NR (2008) Chlorophyll fluorescence: a probe of photosynthesis in vivo. *Annu Rev Plant Biol* 59:89–113
- Basu S, Roy AS, Mohanty K, Ghoshal AK (2013) Enhanced CO₂ sequestration by a novel microalga: *Scenedesmus obliquus* SA1 isolated from bio-diversity hotspot region of Assam, India. *Bioresour Technol* 143:369–377
- Bernacchi CJ, Morgan PB, Ort DR, Long SP (2005) The growth of soybean under free air [CO₂] enrichment (FACE) stimulates photosynthesis while decreasing in vivo Rubisco capacity. *Planta* 220:434–446
- Bhola VK, Swalaha FM, Nasr M, Kumari S, Bux F (2016) Physiological responses of carbon-sequestering microalgae to elevated carbon regimes. *Eur J Phycol* 51:401–412
- Black MT, Brearley TH, Horton P (1986) Heterogeneity in chloroplast photosystem II. *Photosynth Res* 8:193–207
- Chiu SY, Kao CY, Chen CH, Kuan TC, Ong SC, Lin CS (2008) Reduction of CO₂ by a high-density culture of *Chlorella* sp. in a semicontinuous photobioreactor. *Bioresour Technol* 99:3389–3396
- Chiu SY, Kao CY, Tsai MT, Ong SC, Chen CH, Lin CS (2009) Lipid accumulation and CO₂ utilization of *Nannochloropsis oculata* in response to CO₂ aeration. *Bioresour Technol* 100:833–838
- Chiu SY, Kao CY, Huang TT, Lin CJ, Ong SC, Chen CD, Chang JS, Lin CS (2011) Microalgal biomass production and on-site bioremediation of carbon dioxide, nitrogen oxide and sulfur dioxide from flue gas using *Chlorella* sp. cultures. *Bioresour Technol* 102:9135–9142
- Cosgrove J, Borowitzka MA (2010) Chlorophyll fluorescence terminology: an introduction. In: Suggett DJ, Prášil O, Borowitzka MA (eds) *Chlorophyll *a* Fluorescence in Aquatic Sciences: Methods and Applications*. Springer, Dordrecht, pp 1–17
- Dao LHT, Beardall J (2016a) Effects of lead on two green microalgae *Chlorella* and *Scenedesmus*: photosystem II activity and heterogeneity. *Algal Res* 16:150–159
- Dao LHT, Beardall J (2016b) Effects of lead on growth, photosynthetic characteristics and production of reactive oxygen species of two freshwater green algae. *Chemosphere* 147:420–429
- De Marchin T, Ghysels B, Nicolay S, Franck F (2014) Analysis of PSII antenna size heterogeneity of *Chlamydomonas reinhardtii* during state transitions. *BBA-Bioenergetics* 1837:121–130
- Eilers PHC, Peeters JCH (1988) A model for the relationship between light intensity and the rate of photosynthesis in phytoplankton. *Ecol Model* 42:199–215
- Falk S, Palmqvist K (1992) Photosynthetic light utilization efficiency, photosystem II heterogeneity, and fluorescence quenching in *Chlamydomonas reinhardtii* during the induction of the CO₂-concentrating mechanism. *Plant Physiol* 100:685–691
- Giordano M, Beardall J, Raven JA (2005) CO₂ concentrating mechanisms in algae: Mechanisms, environmental modulation, and evolution. *Annu Rev Plant Biol* 56:99–131
- Guenther JE, Melis A (1990) The physiological significance of photosystem II heterogeneity in chloroplasts. *Photosynth Res* 23:105–109
- Henley WJ (1993) Measurement and interpretation of photosynthetic light-response curves in algae in the context of photoinhibition and diel changes. *J Phycol* 29:729–739
- Henley WJ (1995) On the measurement and interpretation of photosynthetic light-response curves in algae in the context of photoinhibition and diel changes. *J Phycol* 31:674
- Ihnken S, Kromkamp JC, Beardall J (2011) Photoacclimation in *Dunaliella tertiolecta* reveals a unique NPQ pattern upon exposure to irradiance. *Photosynth Res* 110:123–137
- Iwasaki I, Kurano N, Miyachi S (1996) Effects of high-CO₂ stress on photosystem II in a green alga, *Chlorococcum littorale*, which has a tolerance to high CO₂. *J Photochem Photobiol B Biol* 36:327–332
- Jianrong XIA, Qiran T (2009) Early stage toxicity of excess copper to photosystem II of *Chlorella pyrenoidosa*–OJIP chlorophyll *a* fluorescence analysis. *J Environ Sci* 21:1569–1574
- Kalaji HM, Schansker G, Ladle RJ, Goltsev V, Bosa K, Allakhverdiev SI, Brestic M, Bussotti F, Calatayud A, Dąbrowski P, Elsheery NI, Ferroni L, Guidi L, Hogewoning SW, Jajoo A, Misra AN, Nebauer SG, Pancaldi S, Penella C, Poli D, Pollastrini M, Romanowska-Duda ZB, Rutkowska B, Seródio J, Suresh K, Szulc

- W, Tambussi E, Yannicari M, Zivcak M (2014) Frequently asked questions about in vivo chlorophyll fluorescence: Practical issues. *Photosynth Res* 122:121–158
- Kamalanathan M, Pierangelini M, Shearman LA, Gleadow R, Beardall J (2016) Impacts of nitrogen and phosphorus starvation on the physiology of *Chlamydomonas reinhardtii*. *J Appl Phycol* 28:1509–1520
- Kyle DJ, Haworth P, Arntzen CJ (1982) Thylakoid membrane protein phosphorylation leads to a decrease in connectivity between photosystem II reaction centers. *Biochim Biophys Acta Bioenerg* 680:336–342
- Lavergne J, Trissl HW (1995) Theory of fluorescence induction in photosystem II: derivation of analytical expressions in a model including exciton-radical-pair equilibrium and restricted energy transfer between photosynthetic units. *Biophys J* 68:2474–2492
- Li T, Tao Q, Di Z, Lu F, Yang X (2015) Effect of elevated CO₂ concentration on photosynthetic characteristics of hyperaccumulator *Sedum alfredii* under cadmium stress. *J Integr Plant Biol* 57:653–660
- Li T, Kirchhoff H, Gargouri M, Feng J, Cousins AB, Pienkos PT, Gang DR, Chen S (2016) Assessment of photosynthesis regulation in mixotrophically cultured microalga *Chlorella sorokiniana*. *Algal Res* 19:30–38
- Ma S, Li D, Yu Y, Li D, Yadav RS, Feng Y (2019) Application of a microalga, *Scenedesmus obliquus* PF3, for the biological removal of nitric oxide (NO) and carbon dioxide. *Environ Pollut* 252:344–351
- Makino A, Mae T (1999) Photosynthesis and plant growth at elevated levels of CO₂. *Plant Cell Physiol* 40:999–1006
- Markou G, Depraetere O, Muylaert K (2016) Effect of ammonia on the photosynthetic activity of *Arthrospira* and *Chlorella*: a study on chlorophyll fluorescence and electron transport. *Algal Res* 16:449–457
- Markou G, Dao LHT, Muylaert K, Beardall J (2017) Influence of different degrees of N limitation on photosystem II performance and heterogeneity of *Chlorella vulgaris*. *Algal Res* 26:84–92
- Masojidek J, Vonshak A, Torzillo G (2010) Chlorophyll *a* fluorescence applications in microalgal mass cultures. In: Suggett DJ, Prášil O, Borowitzka MA (eds) *Chlorophyll a Fluorescence in Aquatic Sciences: Methods and Applications*. Springer, Dordrecht, pp 277–292
- Maxwell K, Johnson GN (2000) Chlorophyll fluorescence—a practical guide. *J Exp Bot* 51:659–668
- Melis A, Neidhardt J, Benemann JR (1998) *Dunaliella salina* (Chlorophyta) with small chlorophyll antenna sizes exhibit higher photosynthetic productivities and photon use efficiencies than normally pigmented cells. *J Appl Phycol* 10:515–525
- Mende D (1980) Evidence for a cyclic PS-II-electron transport in vivo. *Plant Sci Lett* 17:215–220
- Müller P, Li X-P, Niyogi KK (2001) Non-photochemical quenching. A response to excess light energy. *Plant Physiol* 125:1558–1566
- Nagase H, Yoshihara KI, Eguchi K, Yokota Y, Matsui R, Hirata K, Miyamoto K (1997) Characteristics of biological NO_x removal from flue gas in a *Dunaliella tertiolecta* culture system. *J Ferment Bioeng* 83:461–465
- Nagase H, Yoshihara K, Eguchi K, Okamoto Y, Murasaki S, Yamashita R, Hirata K, Miyamoto K (2001) Uptake pathway and continuous removal of nitric oxide from flue gas using microalgae. *Biochem Eng J* 7:241–246
- Nedbal L, Trtílek M, Kaftan D (1999) Flash fluorescence induction: a novel method to study regulation of photosystem II. *J Photochem Photobiol B Biol* 48:154–157
- Pierangelini M, Stojkovic S, Orr PT, Beardall J (2014a) Photosynthetic characteristics of two *Cylindrospermopsis raciborskii* strains differing in their toxicity. *J Phycol* 50:292–302
- Pierangelini M, Stojkovic S, Orr PT, Beardall J (2014b) Elevated CO₂ causes changes in the photosynthetic apparatus of a toxic cyanobacterium, *Cylindrospermopsis raciborskii*. *J Plant Physiol* 171:1091–1098
- Qiu B, Gao K (2002) Effects of CO₂ enrichment on the bloom-forming cyanobacterium *Microcystis Aeruginosa* (Cyanophyceae): Physiological responses and relationships with the availability of dissolved inorganic carbon. *J Phycol* 38:721–729
- Ralph PJ, Gademann R (2005) Rapid light curves: a powerful tool to assess photosynthetic activity. *Aquat Bot* 82:222–237
- Raven JA, Beardall J, Giordano M (2014) Energy costs of carbon dioxide concentrating mechanisms in aquatic organisms. *Photosynth Res* 121:111–124
- Ruban AV, Johnson MP, Duffy CDP (2011) Natural light harvesting: principles and environmental trends. *Energy Environ Sci* 4:1643–1650
- Schmitz P, Maldonado-Rodriguez R (2001) Evaluation of the modulated status of *Vigna unguiculata* probed by the JIP test based on the chlorophyll *a* fluorescence rise. In: 12th International Photosynthesis Congress. Brisbane, Australia,
- Seböck S, Herppich WB, Hanelt D (2017) Red alga *Palmaria palmata*—growth rate and photosynthetic performance under elevated CO₂ treatment. *J Appl Phycol* 29:381–393
- Seth JR, Wangikar PP (2015) Challenges and opportunities for microalgae-mediated CO₂ capture and biorefinery. *Biotechnol Bioeng* 112:1281–1296
- Spalding MH, Critchley C, Govindjee, Orgren WLO (1984) Influence of carbon dioxide concentration during growth on fluorescence induction characteristics of the green alga *Chlamydomonas reinhardtii*. *Photosynth Res* 5:169–176
- Stirbet A, Govindjee SBJ, Strasser RJ (1998) Chlorophyll *a* fluorescence induction in higher plants: modelling and numerical simulation. *J Theor Biol* 193:131–151
- Strasser RJ, Srivastava A, Govindjee (1995) Polyphasic chlorophyll *a* fluorescence transient in plant and cyanobacteria. *Photochem Photobiol* 61:32–42
- Strasser RJ, Tsimilli-Michael M, Srivastava A (2004) Analysis of the chlorophyll *a* fluorescence transient. In: Papageorgio GC, Govindjee (eds) *Chlorophyll a Fluorescence: A Signature of Photosynthesis*. Springer, Dordrecht, pp 321–362
- Tchernov D, Hassidim M, Vardi A, Luz B, Sukenik A, Reinhold L, Kaplan A (1998) Photosynthesizing marine microorganisms can constitute a source of CO₂ rather than a sink. *Can J Bot* 76:949–953
- Varshney P, Mikulic P, Vonshak A, Beardall J, Wangikar PP (2015) Extremophilic micro-algae and their potential contribution in biotechnology. *Bioresour Technol* 184:363–372
- Varshney P, Sohoni S, Wangikar PP, Beardall J (2016) Effect of high CO₂ concentrations on the growth and macromolecular composition of a heat- and high-light-tolerant microalga. *J Appl Phycol* 28:2631–2640
- Varshney P, Beardall J, Bhattacharya S, Wangikar PP (2018) Isolation and biochemical characterisation of two thermophilic green algal species- *Asterarcys quadricellulare* and *Chlorella sorokiniana*, which are tolerant to high levels of carbon dioxide and nitric oxide. *Algal Res* 30:28–37
- Vincent WF, Roy S (1993) Solar ultraviolet-B radiation and aquatic primary production: Damage, protection, and recovery. *Environ Rev* 1:1–12
- Vinet L, Zhedanov A (2011) A ‘missing’ family of classical orthogonal polynomials. *J Phys A Math Theor* 44:085201
- Yang Y, Gao K (2003) Effects of CO₂ concentrations on the freshwater microalgae, *Chlamydomonas reinhardtii*, *Chlorella pyrenoidosa* and *Scenedesmus obliquus* (Chlorophyta). *J Appl Phycol* 15:379–389
- Yoshihara K-I, Hiroyasu N, Eguchi K, Hirata K (1996) Biological elimination of nitric oxide and carbon dioxide from flue gas by marine microalga NOA-13 cultivated in a long tubular photobioreactor. *J Ferment Bioeng* 82:351–354

- Zhang D, Pan X, Mu G, Wang J (2010a) Toxic effects of antimony on photosystem II of *Synechocystis* sp. as probed by in vivo chlorophyll fluorescence. *J Appl Phycol* 22:479–488
- Zhang T, Gong H, Wen X, Lu C (2010b) Salt stress induces a decrease in excitation energy transfer from phycobilisomes to photosystem II but an increase to photosystem I in the cyanobacterium *Spirulina platensis*. *J Plant Physiol* 167:951–958
- Zhang S, Pei H, Hu W, Qi F, Han L, Song M, Han F (2015) Biomass and lipid accumulation of three new screened microalgae with high concentration of carbon dioxide and nitric oxide. *Environ Technol* 36: 2278–2284
- Zhao B, Wang J, Gong H, Wen X, Ren H, Lu C (2008) Effects of heat stress on PSII photochemistry in a cyanobacterium *Spirulina platensis*. *Plant Sci* 175:556–564
- Zhao B, Su Y, Zhang Y, Cui G (2015) Carbon dioxide fixation and biomass production from combustion flue gas using energy microalgae. *Energy* 89:347–357

Publisher's note Springer Nature remains neutral with regard to jurisdictional claims in published maps and institutional affiliations.